Thesis work for the degree of Licentiate of Technology Sundsvall 2012

Analysis and Implementation of Switch Mode Power Supplies in MHz Frequency Region

Abdul Majid

Supervisors: Associate Professor Kent Bertilsson

Professor Bengt Oelmann

Electronics Design Division, in the Department of Information Technology and Media Mid Sweden University, SE-851 70 Sundsvall, Sweden

ISSN 1652-8948 Mid Sweden University Licentiate Thesis 80

ISBN 978-91-87103-13-1





Akademisk avhandling som med tillstånd av Mittuniversitetet i Sundsvall framläggs till offentlig granskning för avläggande av teknologie Licentiate examen i elektronik onsdagen den 14 Juni , klockan 10:15 i sal O111 , Mittuniversitetet Sundsvall. Seminariet kommer att hållas på engelska.

Analysis and Implementation of Switch Mode Power Supplies in MHz Frequency Region

Abdul Majid

© Abdul Majid, 2012

Electronics Design Division, in the Department of Information Technology and Media Mid Sweden University, SE-851 70 Sundsvall Sweden

Telephone: +46 (0)60 148705

Printed by Kopieringen Mittuniversitetet, Sundsvall, Sweden, 2012

ABSTRACT

A power supply is an essential part of almost every electronic device and the current trend is towards the miniaturization of these devices. It is thus desirable to also attempt to reduce the size of the power supply and it is possible to achieve this objective by increasing the power density which is attainable by decreasing the size of the passive/energy storage components such as the inductors, capacitors and the transformer. The size of these components can also be decreased by increasing the switching frequencies.

Linear power supplies use bulky line frequency transformers and heat sinks and are thus not capable of providing a significant opportunity to reduce their size and weight. Switch Mode Power Supplies (SMPS) use higher switching frequencies, which replaces the bulky line frequency magnetics by smaller high frequency magnetics which are then able to offer significant size and weight reductions. The efficiency and size of the SMPS depends on a suitable switching frequency.

Previously, the SMPS were implemented using bipolar power devices and their switching frequency range was limited to a range of a few kHz. With the availability of modern and efficient power MOSFETs, it is possible to switch the SMPS from several kHz to a MHz range. In addition, core based transformers were previously used in SMPS. These transformers have hysteresis and eddy current losses. Their switching frequency was limited to several hundreds of kHz. Recent research has produced energy efficient multilayered PCB transformers which can be implemented in SMPS for power and signal transfer applications, in the MHz frequency range. Thus, with the emerging power devices in GaN and SiC technology and the development of high frequency multilayered PCB power transformers, it is now possible to design high frequency and power efficient isolated converters.

The focus of the research is to design, implement and evaluate energy efficient AC-DC and DC-DC isolated converter topologies. These converters are designed by using the latest power electronic devices and PCB transformers. They are switched in the MHz frequency range.

In this thesis, two DC-DC converters, half bridge and full bridge, are designed, implemented and evaluated. These converters are switched in the MHz frequency range. The energy efficiency of the converter is measured and analysed by varying different circuit parameters. Feedback analysis is made in the case of the Half Bridge converter. The opto-coupler and auxiliary feedback techniques are implemented, measured and analysed in a high frequency half bridge converter using a PCB power transformer. The feasibility of the feedback signal, using the auxiliary winding of a PCB power transformer, is discussed.

The multilayered PCB transformers used in the converter circuits have provided a major contribution with regards to both the energy efficiency and size compactness. This research work is a initial step in the design, implementation and analysis of SMPS operating in the MHz frequency region, using PCB transformers.

ACKNOWLEDGEMENTS

Countless thanks to ALLAH Almighty, the Creator of all of us, worthy of all praise, Who guides us in darkness and helps us in difficulties; who enabled me to work on this thesis and complete it.

I am deeply indebted to my supervisors Dr. Kent Bertilsson and Prof. Bengt Oelmann for their kind support and valuable guidance. The help, encouragement and motivation provided by Dr. Kent Bertilsson is gratefully acknowledged. His enthusiasm and immense knowledge helped me in all times of research and writing of this thesis.

I express my gratitude to my fellow research group members, Jawad Saleem, Hari Babu Kotte and Radhika Ambadipudi for their help motivation and expert opinions.

I am very grateful to my friends Naeem Ahmad, Khurram Shahzad, Khursheed, Abdul Waheed Malik, Muhammad Imran, Mazhar Hussain, Muhammad Amir Yousaf and Anzar Alam, for their help and motivation.

I acknowledge my colleagues Stefan Haller, Fanny Burman, Lotta Söderström, Krister Alden, Benny Thörnberg, Class Mattsson, Cheng Peng, Najeem Lawal, and Sebestian Bader.

I acknowledge the Higher Education Commission and Mid Sweden University for their financial support.

My sincere thanks go to my parents, brothers and sisters who have encouraged and prayed for me during my studies. Thanks to my younger sister Amina Jabeen, who visited me to take care of my children. With her help I was able to spend more time on my research work.

Finally, I am very thankful to my wife Dr. Shazia Jamil for her unconditional cooperation and untiring support throughout the years of my studies. I am thankful to my delightful and cute children, Muhammad Talha, Muhammad Zubair and Madeeha Ftima for taking away all my day-time worries with their innocent smiles.

Sundsvall, May 2012

TABLE OF CONTENTS

| A | BSTRACT | III |
|---|---|------|
| A | CKNOWLEDGEMENTS | V |
| A | BBREVIATIONS AND ACRONYMS | IX |
| L | IST OF FIGURES | XI |
| L | IST OF TABLES | XIII |
| L | IST OF PAPERS | XV |
| | HESIS OUTLINE | |
| 1 | INTRODUCTION | |
| - | | |
| | 1.1 LINEAR VERSUS SWITCH MODE POWER SUPPLIES | |
| | 1.2.1 High frequency power electronic devices | |
| | 1.2.1 High frequency power electronic devices | |
| | 1.2.3 EMI filter size reduction | |
| | 1.3 CHALLENGES IN HIGH FREQUENCY CONVERTER DESIGN | |
| | 1.4 MAIN FOCUS OF THE THESIS | |
| 2 | HALF BRIDGE CONVERTER | |
| | 2.1 TRANSFORMER DESIGN FOR HALF BRIDGE CONVERTER | 9 |
| | 2.2 MULTILAYERD PCB TRANSFORMERS | 9 |
| | 2.2.1 Parameters of PCB transformer | |
| | 2.2.2 Energy efficiency of the transformer | |
| | 2.3 SIMULATION MODEL OF HALF BRIDGE CONVERTER | |
| | 2.4 HARDWARE IMPLEMENTATION | |
| | 2.5 MEASUREMENT RESULTS OF THE CIRCUIT | |
| | 2.6 LOSS ESTIMATION OF HALF BRIDGE CONVERTER | 16 |
| 3 | FEED-BACK TECHNIQUES IMPLEMENTED IN HALF BRIDGE CONVERTER | 10 |
| | | |
| | 3.1 DESCRIPTION OF FEEDBACK CIRCUIT | |
| | 3.1.1 Opto-coupler feedback | |
| | 3.1.2 Auxiliary feedback | |
| 4 | FULL BRIDGE CONVERTER DESIGN | 25 |
| | 4.1 SIMULATION MODEL | |
| | 4.2 HARDWARE IMPLEMENTATION AND MEASUREMENT RESULTS | |
| | 4.3 PARAMETERS OF PCB TRANSFORMER USED IN FULL BRIDGE CONVERTER | |
| | 4.4 DESIGN LIMITATIONS | 28 |
| 5 | THESIS SUMMARY AND CONCLUSIONS | 29 |
| | 5.1 FUTURE WORK | 30 |

| 6 | PAPER SUMMARY | 31 |
|----|--|---------|
| | 6.1 HIGH FREQUENCY HALF-BRIDGE CONVERTER USING MULTILAYERED | |
| | CORELESS PRINTED CIRCUIT BOARD STEP-DOWN POWER TRANSFORMER | 31 |
| | 6.2 ANALYSIS OF FEEDBACK IN CONVERTER USING CORELESS PRINTED CIRCUIT | |
| | BOARD TRANSFORMER | 31 |
| | 6.3 HIGH FREQUENCY FULL BRIDGE CONVERTER USING MULTILAYER CORELESS | |
| | PRINTED CIRCUIT BOARD STEP UP POWER TRANSFORMER PLATFORM | |
| | 6.4 AUTHORS' CONTRIBUTIONS | 33 |
| R | EFERENCES | 34 |
| PA | APER I ERROR! BOOKMARK NOT DEFINE | ED. |
| | HIGH FREQUENCY HALF-BRIDGE CONVERTER USING MULTI-LAYERED CORELESS PRINTED CIRCUIT BOARD STEP-DOWN POWER TRANSFORMER ERROR! BOOKMARK NOT | DEFINED |
| PA | APER II ERROR! BOOKMARK NOT DEFINE | ED. |
| | ANALYSIS OF FEEDBACK IN CONVERTER USING CORELESS PRINTED CIRCUIT BOARD | |
| | TRANSFORMER ERROR! BOOKMARK NOT DEFIN | ED. |
| PA | APER III ERROR! BOOKMARK NOT DEFINE | ED. |
| | HIGH FREQUENCY FULL BRIDGE CONVERTER USING MULTILAYER CORELESS PRINTED CIRCUIT ROARD STEP LIP POWER TRANSFORMER ERROR! BOOKMARK NOT DEFIN | ED. |

ABBREVIATIONS AND ACRONYMS

EMI Electro Magnetic Compatibility

EMI Electro Magnetic Interference

HEMT High Electron Mobility Transistors

IR Infra-Red

GaN Gallium Nitride
LED Light Emitting Diode

MOSFET Metal Oxide Semiconductor Field Effect Transistor

PCB Printed Circuit Board
PWM Pulse Width Modulation

SiC Silicon Carbide

SMPS Switch Mode Power Supplies ZVS Zero Voltage Switching

LIST OF FIGURES

| Figure 1 Linear Power Supply Block diagram | 1 |
|---|------|
| Figure 2 Block diagram of Switch Mode Power Supply | 2 |
| Figure 3 Half Bridge Converter [5] | |
| Figure 4 Coreless PCB Transformer | |
| Figure 5 Energy efficiency of power transformer used in the converter circuit [21]. | .11 |
| Figure 6 Circuit diagram of half bridge converter | . 12 |
| Figure 7 Simulated Gate Signals for high side and low side MOSFETs | . 12 |
| Figure 8 Measured Gate signals for MOSFETs | . 13 |
| Figure 9 Measured Gate signals with two MOSFET drivers | . 14 |
| Figure 10 Energy efficiency as a function of output power | . 15 |
| Figure 11 Energy efficiency as a function of switching frequency | . 16 |
| Figure 12 Thermal profile of MOSFETS | . 18 |
| Figure 13 Thermal profile of rectifier diode | . 18 |
| Figure 14 Opto-coupler diagram | . 20 |
| Figure 15 Schematic diagram of half bridge converter using opto-coupler feedback | . 21 |
| Figure 16 Variation of Vopto with variation of Vout for different loads | . 21 |
| Figure 17 Schematic diagram of half bridge converter using auxiliary feedback | . 22 |
| Figure 18 Variation of Vaux with Vout for different loads | . 23 |
| Figure 19 Variation of input current with V _{out} for different loads | . 24 |
| Figure 20 Measured and calculated values of V _{out} | . 24 |
| Figure 21 Full Bridge converter[5] | . 25 |
| Figure 22 Schematic diagram of full bridge converter | . 26 |
| Figure 23 Variation of energy efficiency with the variation of switching frequency. | . 27 |
| Figure 24 Energy efficiency of the coreless PCB power transformer | . 28 |
| Figure 25 Thermal profile of MOSFETs | . 28 |

LIST OF TABLES

| Table 1 Comparison | of different power | supply technologies | [2] | 3 |
|----------------------|--------------------|---------------------|-----|----|
| Table 13-1. Authors' | Contributions | | | 33 |

LIST OF PAPERS

This thesis is mainly based on the following three papers, herein referred to by their Roman numerals:

Paper I High Frequency Half-Bridge Converter using Multilayered Coreless Printed Circuit Board Step-Down Power Transformer

A.Majid, H.B.Kotte, J.Saleem, R.Ambatipudi, S.Haller, K.Bertilsson

Proceedings of 8th Internal Conference on Power Electronics-ICPE 2011 at Jeju South Korea (May 28-June 03 2011)

Paper II Analysis of Feedback in Converter using Coreless Printed Circuit Board Transformer

A.Majid, J.Saleem, H.B.Kotte, R.Ambatipudi, S.Haller, K.Bertilsson

Proceedings of International Aegean Conference on Electrical Machines and Power Electronics & Electromotion-ACEMP 2011 at Turkey Istambul (September 08-10, 2011)

Paper III High Frequency Full Bridge Converter using Multilayer Coreless Printed Circuit Board Stepup Power Transformer

J.Saleem, A. Majid, R.Ambatipudi, H. B. Kotte,

K. Bertilsson

Proceedings of 20th European Conference on Circuit Theory and Design Linköping Sweden August 29- 31,2011

Papers not included in this thesis

Paper IV Study the influence of the alignment and nearby metallic objects on the Hall sensor system for current measurement

in Resistance Spot Welding Machine.

J.Saleem, A. Majid, K.Bertilsson, Linda Schuberg

Proceedings of International Conference on Environment and Electrical Engineering 2011Rome Italy 8th May—11th May 2011

Paper V A Study of IGBT Rupture Phenomenon In Medium Frequency Spot Welding Machine.

J.Saleem, A. Majid, S. Haller, K. Bertilsson

Proceedings of International Aegean Conference on Electrical Machines and Power Electronics & Electromotion-ACEMP 2011 at Turkey Istambul (September 08-10, 2011)

THESIS OUTLINE

Chapter 1: This chapter provides brief introduction of linear and switch mode power supplies. Design issues of high frequency SMPS are discussed.

Chapter 2: In this chapter the design of half bridge converter is discussed. The simulation results are discussed. The energy efficiency of the converter is computed by varying various circuit parameters.

Chapter 3: This chapter is mainly focused on the feedback control techniques used in half bridge converter. Two feedback techniques are analysed. In the first technique the opto-coupler is used on the secondary side of the converter and in the second technique the auxiliary winding of the transformer is used for the feedback signals.

Chapter 4: The design of high frequency full bridge DC-DC converter using coreless PCB step-up transformer is discussed in this chapter

Chapter 5: presents a papers summary.

Papers which are basis for this research work are listed at the end.

1 INTRODUCTION

A power supply is an essential part of every electronic device. It converts an AC power line voltage to a steady state DC output voltage as required by all electronic circuits. Power supplies can be categorized into two types: linear and Switch Mode.

The block diagram of a linear regulated power supply is shown in Figure 1. It consists of a transformer, rectifier, and filtering and regulator circuits. The rectifiers are used to convert 50/60Hz AC voltage to a pulsating DC. The filters are used to convert the pulsating DC to a smooth voltage. Finally, the voltage regulators are used to produce a constant output voltage, irrespective of the variations in the ac line voltage or by the circuit loadings. The output voltage is sampled by an error amplifier block which compares it with a reference signal and generates an error signal on the basis of comparison. The error signal is applied to a series pass element which alters its resistance accordingly and thus regulates the output voltage. Hence, the series pass element absorbs any changes in the input voltage and any dynamic changes in the output voltage due to the load changes, within its designed tolerance band [1]. The size of the components, such as the transformers and output filters, are very bulky in these supplies. Linear power supplies are not suitable for smaller modern electronics system because of their high power loss, low power density and bulky size.

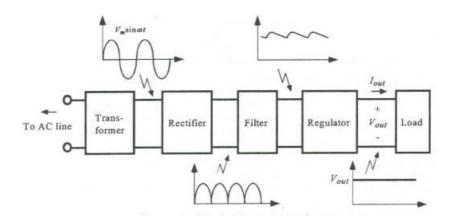


Figure 1 Linear Power Supply Block diagram

Like linear power supplies, the SMPS converts the available unregulated AC or DC input to a regulated DC output. The input is taken from the AC mains and then rectified, filtered and fed to a high frequency DC-DC converter. SMPS can be operated within the kHz to MHz frequency range. The increased switching frequencies cause a decrease in the size of the energy storage elements, such as the capacitors, inductors and transformers, in an almost linear manner. SMPS is further divided into two types: isolated and non-isolated.

Common examples of non-isolated switch mode power supply topologies are the buck, boost and the buck-boost converters. This type is a common building block for many complex power supply topologies. This type is the simplest and requires less components in comparison to those for isolated supplies.

In an isolated type, a high frequency transformer is used to isolate the output from the input, scale the output voltage magnitude with turn ratio and to produce the multiple DC outputs. Large step-up or step down ratios can be achieved in converters by using a transformer. The voltage/current stresses on transistors and diodes can be minimized by means of the correct choice of transformer turn ratio.

The block diagram of an isolated SMPS circuit is shown in Figure 2.

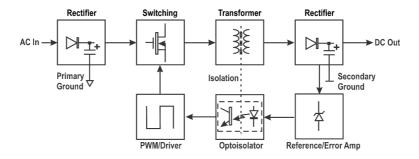


Figure 2 Block diagram of Switch Mode Power Supply

1.1 LINEAR VERSUS SWITCH MODE POWER SUPPLIES

The linear power supplies are bulky and less efficient in comparison to those of SMPS. In high current equipment, the size of linear power supplies becomes larger because of the Mains-frequency transformer and the large sized heat sink. Each linear regulator has an average energy efficiency of 35% to 50% and the losses are dissipated as heat [2]. However, the linear regulated supplies have better performance when compared with SMPS in terms of line and load regulations, output ripple, EMI, transient recovery and hold up time requirements [3].

The SMPS are much more efficient and flexible than the linear regulators and it is possible to achieve a high energy density by using them. They are portable and are commonly used in aircrafts products, laptop adaptors, off line applications and small instruments. Due to their smaller size they require less heat-sinking for the same output power as compared to that for linear power supplies. The PWM SMPS are switched at a very high frequency and at these frequencies, especially at high voltages, the switching losses increase and thus limit the performance of the supply. To overcome this problem, different soft switching techniques are often used and resonant and quasi resonant switching power supplies are emerging. Recent research has focused on the design of low profile, energy efficient and compact switch mode power supplies.

Although both linear and switch mode power supplies perform the same function of converting an unregulated input voltage to a regulated output voltage but they have significant differences in their properties and performance. The important differences are mentioned below [4][5]:

- Linear regulators exhibit energy efficiency of 20 to 60% while SMPS have energy efficiency of 75-95%.
- The SMPS transformers are subjected to the non-sinusoidal input/output currents and voltages, whereas the transformers in linear supplies are subjected to sinusoidal voltages and currents.

A comparison of different power supplies is given in Table 1.

| | Linear | PWM switching | Resonant switching | Quasi-Resonant |
|------------|------------|---------------|--------------------|----------------------|
| | Regulators | regulators | regulators | switching regulators |
| Cost | Low | High | High | High |
| Mass | High | Low-medium | Low-medium | Low-medium |
| RF Noise | None | High | Medium | Medium |
| Efficiency | 35-50% | 70-85% | 78-92% | 78-92% |
| Multiple | No | Yes | Yes | Yes |
| outputs | | | | |
| Complexity | Less | Medium | High | High |

Table 1 Comparison of different power supply technologies [2]

1.2 MOTIVATION FOR USING HIGHER SWITCHING FREQUENCIES

New devices and topologies are the driving force behind the development of power electronics. By increasing the switching frequency of the converter, it becomes possible to reduce the size of the SMPS which is a desirable feature. The main objective of this trend is to increase the power density and to improve the dynamic performance of the converter by decreasing the size of the passive components such as inductors, capacitors and transformer [6]. The motivating factors behind the design of high frequency SMPS are based on the fabrication of high frequency power electronic devices and PCB power transformers.

1.2.1 High frequency power electronic devices

The CoolMOS Power MOSFETs offer significant advantages at high power levels. They can be operated with the lowest control power, cheapest drive circuitry and the highest switching frequencies. These are suitable for applications including efficient power supplies and low power applications such as for a battery charger, line adapter and auxiliary supplies [7].

A great achievement from the development in power semiconductors is the wide band-gap technology and the related power devices. Silicon Carbide (SiC) is an emerging semiconductor material and offers a higher breakdown voltage, thermal conductivity, saturated electronic drift velocity and higher junction temperature operation [8].

Gallium Nitride (GaN) is another emerging semiconductor material and GaN-based semiconductors devices have the capability of high-power switching with sub-microsecond and nano-second times. They are suitable for high power and high temperature applications. These devices have high electron mobility and saturation velocity, high sheet carrier concentration at hetero-junction interfaces, high breakdown voltages, and low thermal impedance [9].

1.2.2 High frequency power transformers:

Multilayered PCB power transformers are highly energy efficient and can be used in SMPS for power transfer applications in MHz frequency range. Recent research has shown that high frequency and high energy efficiency of the step down power transformers is possible [10].

Hence, with the fabrication of efficient high frequency electronic devices and with the design of high frequency multilayered PCB power transformers it is now possible to design high frequency and power efficient isolated converters.

1.2.3 EMI filter size reduction

The increased switching frequency in combination with sudden changes in current (di/dt) or voltage(dv/dt) levels generates higher order harmonics. It produces EMI and affects the Electro Magnetic Compatibility (EMC) of the SMPS. It is extremely important to take EMC into consideration during the design phase of the SMPS. The line filter are used for suppressing conducted EMI and in general, the size of the filter is expected to decrease with increasing switching frequency of the SMPS.

1.3 CHALLENGES IN HIGH FREQUENCY CONVERTER DESIGN

Designing the high frequency power converter with a better energy efficiency and reliability is a challenging task as there are more effects caused by the switching frequency on power-supply system than merely on its size and efficiency. The designers encounter severe challenges in relation to the best approach for minimizing the influential factors and optimizing the types and values of the components.

There is always a trade-off between size, cost, weight and energy efficiency of power supplies. If one parameter is solved, then the problem shifts to other parameters. For instance, the improvement in power density of SMPS is achieved by reducing the size of passive components, but this reduction in size demands a higher switching frequency which in turn results in switching losses. The eventual effect is reduced energy efficiency. Although, there are some topologies, e.g. resonant converters, which are used to reduce the switching losses at higher switching frequencies the design of these topologies becomes complicated for large line and load variations. Hence, it becomes difficult to control and stabilize the output voltage. At megahertz frequencies, the semiconductor switch experiences high stress which results in a switching loss.

Although GaN HEMT device structure exhibits better characteristics when compared to silicon-based devices, but the gate drive design for GaN is complex because the internal parasitic capacitances of the devices must be comprehensively considered. The Miller capacitance (C_{GD}) is a nonlinear function of voltage and it causes the total dynamic input capacitance to become greater than the sum of the static capacitances. It slows the turn-on and turn-off transition time of the transistor. It is a source of instability and dv/dt turn on problems [11]. There are driving constraints due to a smaller C_{GD} in GaN MOSFETs. The presence of fast dv/dt together with an unfavorable ratio between the C_{GS} and C_{GD} increases the risk of a Miller turn-on and a short-through in half bridge converters [12]. The proportional relationship between the switching frequency and switching loss in semiconductor devices is another factor to consider. The increase in switching frequency will also increase the power loss. Thus, it becomes more challenging to design a high frequency converter [14].

The influence of parasitic elements, thermal analysis and on-board PCB layout design are important in order to achieve compact, higher power density and high efficient converters.

1.4 MAIN FOCUS OF THE THESIS

The main objective of this thesis is to study the feasibility of energy efficient DC-DC converters in the switching frequency range of MHz. At a higher switching frequency the design of a transformer becomes a challenge. Recently multi-layered PCB transformers have been designed at Mid Sweden University. The geometrical and electrical parameters of different multi-layered PCB transformers are discussed in [10],[13],[20] & [21]. These transformers are much smaller in size as compared to the core based transformers. The energy efficiency of these transformers is more than 90% in the MHz frequency region. Based on their smaller size, high energy density and better energy efficiency, they can be implemented in SMPS for power and signal transfer applications, in the MHz frequency range.

These multi-layered coreless PCB transformers are used in different converter circuits and have offered major contribution in terms of energy efficiency and size compactness of the converters [3].

The focus of this thesis is to use these multi-layered PCB transformers in the implementation of converter circuits. These converters are switched in the MHz frequency range. The transformers are used in step-down and step-up configurations. The energy efficiency of the converters is computed by varying different circuit parameters. Different feedback schemes are studied and implemented in the converters.

In the design process, the converter is analyzed by simulating the model using a circuit simulation tool. The energy efficiency of the converter is computed by varying the circuit parameters. The circuit components are optimized and after a successful evaluation of the converters the prototype is built with integrated PCB power and signal transformers.

2 HALF BRIDGE CONVERTER

Half bridge converter circuits can be used in various applications such as power supplies and motor drives and they are popular choice of converters upto several hundred watts. A half bridge converter has two power switches that operate alternately to produce a square wave AC at the input of the power transformer and are subjected to a voltage stress equal to the input voltage. Two equal sized capacitors are used on the primary side to provide a DC bias in order to balance the volt-second integrals of the two switching intervals. Because of these capacitors the transformer sees a positive and negative voltage during switching which results in twice the desired peak flux value of the core. Two rectifier diodes are used on secondary side, which provide the rectification when one of the power switches is on and act as freewheeling diodes during the time that both power switches are off.

The transformer core is operated in the first and third quadrants of the B-H loop and experiences twice the flux excursion of a similar forward converter core. A half bridge converter utilizes the full available flux swing in both quadrants of the B-H loop, therefore the primary transformer winding has half the turns for the same input voltage and power [15].

Although, the structure of the half bridge circuit is complicated because isolated gate drive signals are required for a high side MOSFET, there are certain advantages to using this topology in DC-DC converter circuits. The advantage of the half bridge converter is that the effective duty cycle, as seen by the input and output filters, is twice that of the individual switch duty cycle. In addition, the effective frequency is twice that of the individual switch frequencies. Both high efficiency and high power density are achievable by using the half bridge converter topology [15]. The problem which occurs in this type of circuits is shoot-through. Shoot-through occurs when both the transistors turn on at the same time, thus creating a short across the main bus. This would be a disaster as it would destroy both the transistors. This situation can occur at turn on, line or load transient, or instability within the closed loop system [16]. The schematic diagram of the half bridge converter is given in Figure 3.

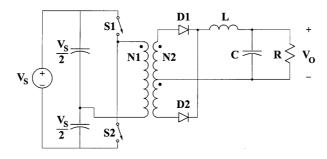


Figure 3 Half Bridge Converter [5]

The operation of the half bridge converter is explained in the following section.

When the power switch S_1 is on and S_2 is off, the primary current Ip quickly ramps up across the leakage inductance and delivers the secondary current. The rectifier diode D_1 is forward biased and D_2 is reverse biased. The energy stored in the primary winding is transferred to the load through the rectifier diode D_1 .

When S1 is turned off, the junction capacitance of switch S2 is charged by the current flowing through the primary winding of the power transformer. After the voltage across the drain-to-source of S2 drops to zero, the body diode of S2 conducts. It provides the path for the energy stored in the leakage inductance of the primary winding. During the body diode conduction period, S2 may be turned on at zero-voltage switching. The magnetizing current that results in the interval during which S_1 is on, flows through the secondary side. The rectifier diode D_2 is forced to conduct while D_1 is already in a conduction state. Hence both D_1 and D_2 conduct during this time and act as freewheeling diodes. They maintain the current flow in the inductor. The magnetizing current is concurrently transferred to the secondary side. Since both D1 and D2 are in parallel, therefore under ideal conditions, an equal amount of current will flow through them and each diode will supply half of the load current. In a practical scenario, the I-V characteristics of both the diodes are not exactly the same and thus the flow of current is slightly different through two rectifier diodes. The inductor current is the sum of the current flowing through both the diodes

When S_2 is turned on and S_1 is off D_2 conducts and D_1 is reversed biased. The output voltage V_0 across the load resistor is given as [5]:

$$V_o = \frac{N_2}{N_1} (Vin \times D)$$
 2.1

where:

 N_1 = Number of turns of primary winding

N₂= Number of turns of secondary winding

D= Duty cycle of Switching waveform

The output power P_{out} is computed according to equation 2.2 below:

$$P_{out} = V_o \times I_I$$
 2.2

The energy efficiency of the converter is given as:

$$\eta = \frac{P_{out}}{P_{in}} \times 100$$

2.1 TRANSFORMER DESIGN FOR HALF BRIDGE CONVERTER

In isolated SMPS the transformer is used to transfer the power efficiently and instantaneously from an external electrical source to an external load. The choice of circuit topology has a great impact on the transformer design. Full bridge and half-bridge topologies offer the best transformer efficiencies because their cores and windings are fully utilized.

There are two main functions of a forward mode transformer:

- It provides galvanic isolation between the input and output.
- It can either step-up or step down the primary voltage.

Ideally, a transformer does not store any energy however in practice, all transformers store some undesired energy:

- Leakage inductance: It represents the energy stored in the non-magnetic regions between the windings, caused by an imperfect flux coupling. In the equivalent electrical circuit, the leakage inductance is in series with the windings.
- Mutual inductance: It represents the energy stored in the finite permeability of
 the magnetic core and in the small gaps where the core halves come together. In
 the equivalent circuit, mutual inductance appears in parallel with the windings.
 The energy stored is a function of the volt-seconds per turn applied to the
 windings and is independent of the load current.

2.2 MULTILAYERD PCB TRANSFORMERS

The high frequency magnetics are the backbone of modern SMPS. In core based transformers, the magnetic cores are used to provide a high degree of magnetic coupling and to reduce the leakage inductance. However these transformers cannot be used for the converters operating in the frequency region of several MHz because of their increased core losses, winding losses and temperature rise. The skin and proximity effects are the major problem in high frequency transformer design. Leakage inductance and unbalanced magnetic flux distribution are two further obstacles for the development of high frequency transformers [17]. PCB transformers have the advantages of low costs, very high power density, no limitation due to magnetic cores, no magnetic loss and ease of manufacturing. They have the potential to be developed in microcircuits [18].

It has been found that coreless PCB transformers can be used for high-frequency operations from about 200 kHz and upwards. The elimination of magnetic cores and the use of printed windings open a new means of manufacturing low-profile transformers with a high power density [19].

The PCB transformers can be used in converters operating in the MHz frequency range. These PCB transformers possess very good high frequency characteristics, and they eliminate the manual winding process. There has been significant research in the design of coreless PCB transformers. These multi-layered coreless PCB transformers are highly

energy efficient [20] and have the potential to be used in both DC-DC and AC-DC converters switching in the MHz frequency region [3].

2.2.1 Parameters of PCB transformer

The 4:1 PCB centre-tapped power transformer, designed for a half bridge converter, is used in the converter. It can be operated in the frequency range of 1 to 6 MHz. The transformer is designed in four layers of PCB and it has two primary windings in the first and fourth layers while there are two secondary windings in the second and third layers. The primary and secondary copper windings of the transformers are etched on the FR4 PCB laminate and, by this means a better coupling between primary and secondary windings is achieved. The primary windings are connected in series and the secondary windings are connected in parallel so as to achieve the desired inductance. The number of turns in the primary winding is 24 and in secondary winding, 6. The electrical parameters of the transformer were measured using an RLC meter at 1 MHz and are:

- The self-inductances of the primary and secondary winding are 7.73μH and 2.33μH respectively.
- The leakage inductances of the primary and secondary winding are 1.38μH and 0.417μH respectively.
- The AC resistance of the primary and secondary windings of the transformer are 2.2Ω and 0.7Ω respectively.
- The inter-winding capacitance is approximately 50pF.

The 4:1 multi-layer coreless PCB power transformer and gate drive transformer used in the circuit are shown in Figure 4.

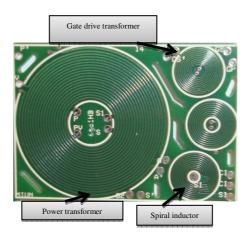


Figure 4 Coreless PCB Transformer

2.2.2 Energy efficiency of the transformer

The maximum gain frequency of a PCB transformer is 8MHz and the maximum impedance frequency is 3.5 MHz with an input impedance of 135Ω . The maximum energy efficiency of the power transformer is approximately 96% at a frequency of 2.6MHz. The power density of the transformer is $16W/cm^2$ [21]. The energy efficiency of this step down power transformer for a load resistance of 10Ω and a sinusoidal excitation up to the output power of 50W is illustrated in Figure 5.

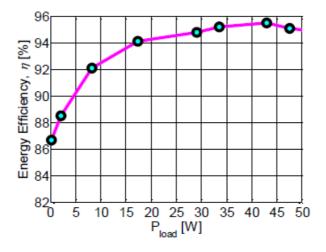


Figure 5 Energy efficiency of power transformer used in the converter circuit [21]

2.3 SIMULATION MODEL OF HALF BRIDGE CONVERTER

The parameters are optimized by simulating the half bridge converter. CoolMOS SPU02N60S5 power MOSFET SPICE model and the power transformer's high frequency model are used in this simulation. The maximum energy efficiency of the converter is computed by variation of the circuit parameters. At best achieved conditions 85 percent energy efficiency is observed in simulations The schematic diagram of the converter is given in Figure 6.

High side and low side MOSFETs are switched alternately. The lower MOSFET is switched directly by a pulsed waveform source while isolation transformer is used for the high side MOSFET. The switching waveforms for driving high and low side MOSFETs are shown in Figure 7.

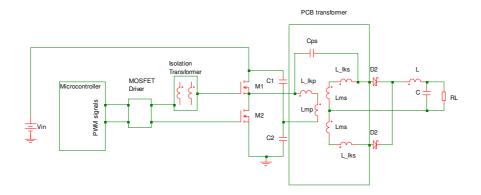


Figure 6 Circuit diagram of half bridge converter

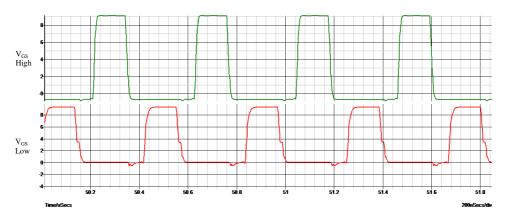


Figure 7 Simulated Gate Signals for high side and low side MOSFETs

2.4 HARDWARE IMPLEMENTATION

A high frequency half bridge converter circuit is implemented on a PCB. The DSPIC33fJ016GS502 microcontroller is used in the converter so as to generate PWM signals that are then fed to a MOSFET driver. It has the following important features and is suitable for medium power converter topologies such as push pull and half bridge converts topologies [22]:

- Individual time base and duty cycle for each of the six outputs of PWM generators
- Duty cycle, dead time, phase shift and frequency resolution of 1.04ns at 40MIPS
- Various PWM modes such as true independent, complementary and fixed off time.

After passing through the driver, the signals are then fed to the gate of the lower MOSFET. To drive the high side MOSFET, a multilayered coreless PCB isolation transformer [20] is used after the gate driver. By using this gate drive transformer, a low power consumption passive gate drive circuitry [3] is built up and utilized to drive the high side MOSFET. Gate signals for the high and low side MOSFETS are shown in Figure 8

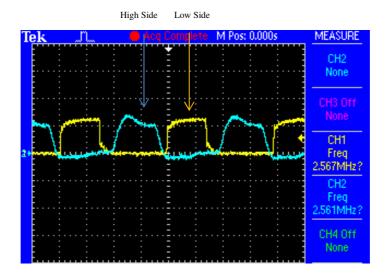


Figure 8 Measured Gate signals for MOSFETs

The rise and fall time of the gate signals for a high side MOSFET is more than that of the low side MOSFET. In order to equalize the rise and fall times of both the high and low side MOSFETs a driver is added into the circuit after the isolation transformer and before the high side MOSFET. The Gate signals for both the high and low side MOSFETs while using two MOSFET drivers, are shown in Figure 9.

The CoolMOS SPU02N60S5 Power MOSFETs M1 and M2 are used in the design. These devices offer significant advantages at high power levels. They can be operated with the lowest control power, the cheapest drive circuitry and the highest switching frequencies [7]. The Drain-Source voltage (V_{DS}) of the MOSFETs is 600 V, $R_{DS(on)}$ is 3 Ω and the continuous drain current (I_D) is 1.8 A. The output capacitance (C_{oss}) of the MOSFET is 77 pF and the total gate charge Qg when V_{DD} 350 V, I_D 1.8 A and V_{gs} 1-10V is 9.5 nC [23].

On the secondary side, the SR 1660 Schottky barrier rectifier diode was used. It has a maximum forward voltage of 0.7~V, an average forward rectified current capability of 16~A and a maximum DC blocking voltage of 60~V [24].

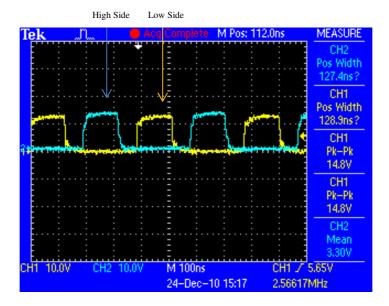


Figure 9 Measured Gate signals with two MOSFET drivers

2.5 MEASUREMENT RESULTS OF THE CIRCUIT

The energy efficiency of the unregulated half bridge converter circuit is computed for the input DC voltage of up-to 170 V and the switching frequency is in the range of 2 to 3 MHz, with different loads and a fixed duty cycle of 30%. The output power of the converter at the maximum input voltage of 170 V is approximately 40 W. When computing the efficiency, the power dissipation of the gate drive circuit is not included. The energy efficiency (η) is computed according to the following expression:

$$\eta = \frac{P_{out}}{P_{in}} \times 100 = \frac{V_{out}^2 / R_L}{V_{in} \times I_{in}} \times 100$$
2.4

The energy efficiency of the converter at a constant 2.5 MHz switching frequency, 30% duty cycle, different loads (10 Ω , 20 Ω and 40 Ω) and for different input voltages is plotted in Figure 10. The converter is tested up-to a maximum output power level of 40 W. At this power level the input voltage is 170V, switching frequency is 2.5 MHz, duty cycle is 30% and the load resistance is 10 Ω .

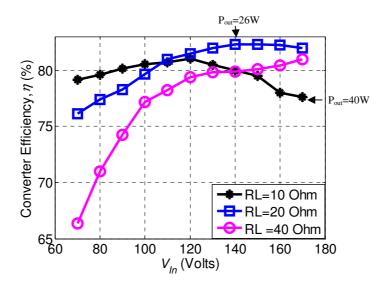


Figure 10 Energy efficiency as a function of output power

The maximum energy efficiency of approximately 82% is obtained at the output power level of 26 W. At this instant the input voltage is 170 V, switching frequency is 2.5 MHz, duty cycle is 30% and the load resistance is 20 Ω . From the measurement results it is observed that there is a degradation in the energy efficiency of the converter as the output power is increased beyond 26 W. At a higher output power and higher switching frequencies, the losses in the semiconductor devices increase and the ZVS conditions of the converter are lost, thus causing a reduction in the energy efficiency.

At higher switching frequencies the stress on the semiconductor devices increases. This results in increased switching losses for the MOSFETs and the rectifier diode and thus causes a reduction in the energy efficiency of the converter.

It is obvious from Figure 11 that as the switching frequency increases beyond 2.8 MHz the energy efficiency significantly reduces. The maximum energy efficiency of the converter is obtained between 2.4 MHz and 2.8 MHz. Below 2.4 MHz the losses in the transformer are dominant, while above 2.8 MHz the switching losses in the MOSFETs are dominant.

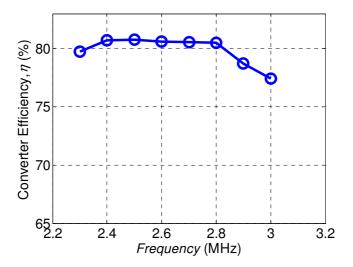


Figure 11 Energy efficiency as a function of switching frequency

2.6 LOSS ESTIMATION OF HALF BRIDGE CONVERTER

From the measurement results presented in section 2.5, it can be observed that as the switching frequency and output power of the converter increases, the energy efficiency degrades due to power losses. The losses are estimated at a 120 V input voltage, 2.5 MHz switching frequency, 30% duty cycle and 10 Ω load resistance. Under these conditions, the input power of the converter is 27 W while, the output power is 22W and thus the total power loss of the converter is about 5 W. These losses in the converter are shared by the MOSFETs, gate driver, power transformer and rectifier diode. The total estimated loss of the power transformer is approximately 2W [25]. The remaining 3W power is lost due to the MOSFETs and the rectifier diode.

MOSFET Losses: There are two categories of losses in the MOSFETs i.e. the conduction loss and the switching loss. The conduction losses in the power MOSFET can be calculated using the on-state resistance (R_{DSon}) of the MOSFET. The required parameters for the conduction loss are R_{DSon} rms current, which flows through the device, and the duty factor. These values are not difficult to quantify and thus the instantaneous value of the MOSFET conduction losses can be computed according to equation 2.5 [26].

$$P_{conduction} = V_{DS} \times I_D = R_{DSon} \times I_D^2(t)$$
 2.5

As shown in equation 2.6 [26], the average value of the MOSFET conduction losses can be computed by the integration of the instantaneous power losses over the switching cycle.

$$P_{con_avg} = \frac{1}{T_{SW}} \int_{0}^{T_{SW}} P_{Con}(t)dt = \frac{1}{T_{SW}} \int_{0}^{T_{SW}} (R_{DSon} \times I_D^2(t))dt = R_{DSon} \times I_{Drms}^2$$
 2.6

The R_{DSon} for CoolMOS SPU02N60S5 is 3 Ω and I_{Drms} is 0.3 A.

According to equation 2.6 the average conduction loss of each MOSFET is 0.4 W.

Switching losses occur as a result of a simultaneous exposure of a MOSFET to high voltage and current during a transition between the open and closed states and is usually difficult to predict. It is difficult to model the complex switching behavior and switching loss of a power MOSFET analytically due to the non-linear characteristics of the MOSFET parasitic capacitances. At higher switching frequencies, the exact estimation of switching is difficult. The impact of the parasitic capacitance and stray inductance also influences the switching losses of the converter.

Since the converter is not fully operated under ZVS conditions, it thus becomes inevitable that there will be a switching. The switching loss of the MOSFETs is estimated to be approximately 1W according to equation 2.7 [27].

$$P_{sw} = \frac{1}{2} I_D \cdot V_{DS} (t_{on} + t_{off}) \cdot f_{SW}$$
 2.7

where:

 I_D is the drain current V_{DS} is the Drain-Source voltage f_{sw} is the switching frequency t_{on} is the turn-on switching time t_{off} is the turn-off switching time

The remaining 1.2W loss is shared by the rectifier diode and other circuit components. From the loss estimations, it is obvious that the MOSFETs are the prominent source of loss within the converter. The temperature profile of the MOSFETs measured using an IR thermal camera is given in Figure 12

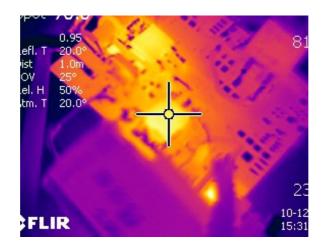


Figure 12 Thermal profile of MOSFETS

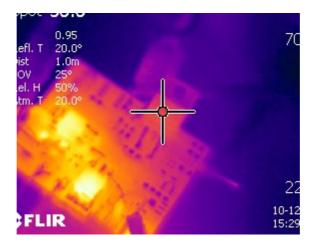


Figure 13 Thermal profile of rectifier diode

Diode Lossess: The output rectifier also contributes to the losses of the converter. Although the Schottky diodes have the lowest forward voltage drop, when this is compared to a normal P-N junction diode, its forward voltage increases more quickly with a higher current. An analysis of the switching loss of the rectifier diode is complicated. The thermal profile of SR-1660 Schottky diode is shown in Figure 13.

3 FEED-BACK TECHNIQUES IMPLEMENTED IN HALF BRIDGE CONVERTER

Almost all power supplies use a feedback loop to achieve a constant DC output voltage. The feedback voltage is applied to the controller, which compares the output voltage with a reference voltage and executes a control algorithm. This control algorithm is used to generate the required PWM signals to drive the MOSFETs. The design of the feedback network is one of the most important aspects of a converter's design. The feedback design is slightly more sophisticated mathematically than other aspects of the power supply design [28]. To design an isolated feedback stage is more challenging than designing an isolated power stage. In a feedback loop, the galvanic isolation is required between the input and output. Various feedback techniques are used in the implementation of an isolated feedback control.

Standard phototransistor opto-couplers are one of the various techniques used to implement an isolated feedback [29], [30]. Although it provides the required isolation, there are several disadvantages when implementing an opto-coupler feedback, such as a variable loop gain due to opto-coupler tolerance and sensitivity to temperature, as well as its relatively high cost.

The other alternatives to that of an opto-coupler feedback are isolated magnetic feedback techniques. The magnetic feedback has good temperature stability and is insensitive to component tolerance [31]. The magnetic feedback implementation on the secondary side of the converter is described in [28]. It provides true high voltage isolation and can be made insensitive to temperature variations.

The auxiliary voltage feedback technique is another alternative to the opto-coupler feedback. It provides a technique to control the output voltage without the need of a feedback circuit on the secondary side of the power supply. The auxiliary voltage feedback has certain advantages as compared to the opto-coupler feedback, such as a higher power density, lower cost and a lower standby power [32].

3.1 DESCRIPTION OF FEEDBACK CIRCUIT

Two feedback techniques are analyzed in the high frequency half bridge converter circuit design. In the first technique an opto-coupler is used on the secondary side and the isolated feed-back signals are analyzed. The variation of the opto-coupler feedback voltage with the variation in the output voltage is measured for different loads.

In the second technique, the feasibility of a feedback signal using the auxiliary winding of a coreless PCB power transformer is discussed. The variation of the auxiliary voltage with the variation of the output voltage for different loads is analyzed.

3.1.1 Opto-coupler feedback

The SMPS require an isolated output voltage control method. The opto-couplers are commonly used to provide an isolated feedback voltage in SMPS [29]. They consist of a

photo-diode that radiates energy proportional to the current flowing through it, and a phototransistor that uses this energy to cause a linearly related collector current. Opto-couplers also offer a high degree of noise rejection or isolation combined with their insulation characteristics [33]. The important parameter for opto-couplers is their transfer efficiency, usually measured in terms of their current transfer ratio (CTR). This is the ratio between a current change in the output transistor and the current change in the input LED which produced it. A diagram of an opto-coupler is shown in Figure 14.

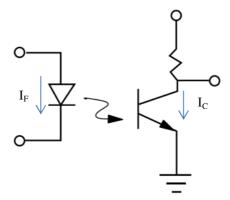


Figure 14 Opto-coupler diagram

The CTR, which is the ratio of the phototransistor collector current to the LED forward current is measured according to equation 3.1.

$$CTR = \frac{I_C}{I_F}$$
 3.1

The opto-coupler feedback technique is implemented in a high frequency half bridge converter. An IL207A opto-coupler is used to provide an isolated feedback voltage V_{opto} . The IL207A opto-couplers are optically coupled pairs with a Gallium Arsenide infrared LED and a silicon NPN phototransistor. They are capable of transmitting signal information, including a DC level, by maintaining a high degree of isolation between the input and output [34]. The isolated feedback voltage V_{opto} is measured at the ADC input of the microcontroller. The variation output voltage V_{out} affects the feedback voltage V_{opto} from the secondary side of the converter. A schematic diagram of the converter with an opto-coupler feedback is shown in Figure 15.

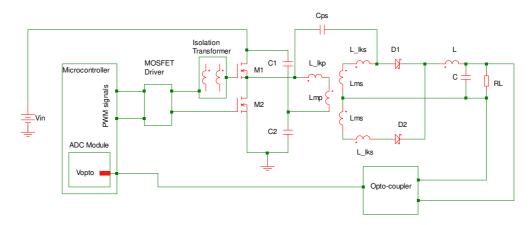


Figure 15 Schematic diagram of half bridge converter using opto-coupler feedback

It is observed that the feedback voltage taken from the opto-coupler varies in proportion to the variation of the output voltage. For a constant output voltage, there is no deviation with the variation of the load resistor. The opto-coupler feedback voltage varies linearly with the variation output voltage as shown in Figure 16.

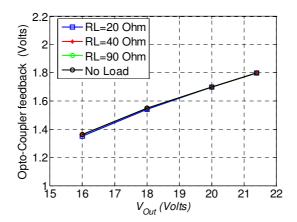


Figure 16 Variation of Vopto with variation of Vout for different loads

3.1.2 Auxiliary feedback

The auxiliary feedback eliminates the need for an opto-coupler on the secondary side and also reduces the device count and the size of the power supply. In strongly coupled transformers the auxiliary voltage is proportional to the output voltage. The variation of the output voltage with varying loads will result in a proportional variation in the voltage

produced by the auxiliary winding [35]. This technique can be used to regulate the output voltage without requiring a secondary feedback in the converter.

The PCB power transformer used in the half bridge converter consists of two number of turns of auxiliary windings in two layers. The inductance of the auxiliary winding is 0.193uH with a DC resistance of 0.42 ohms. The auxiliary winding of the power transformer is strongly coupled with its primary winding.

The voltage taken across the auxiliary winding of transformer is rectified, filtered and applied to a voltage divider in order to obtain the desired value. The schematic diagram of a half bridge converter with auxiliary feedback is shown in Figure 17. The resistors R_1 and R_2 are used to scale down the auxiliary voltage to the voltage levels of the controller ADC input. The voltage across R_2 is measured as an auxiliary feedback voltage.

The shunt resistor R_{shunt} is used in series with the lower MOSFET so as to measure the input current. The input current in combination with the auxiliary feedback voltage is required to accurately predict the output voltage of the converter.

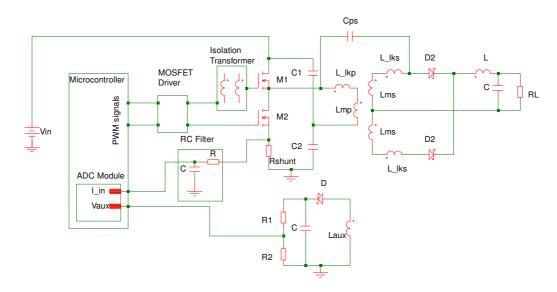


Figure 17 Schematic diagram of half bridge converter using auxiliary feedback

In the auxiliary feedback design, the variation of feed-back voltage V_{aux} is measured with the variation of the following circuit parameters:

- Fixed value of output voltage V_{out} and different values of load resistors.
- Variation of output voltage V_{out} and constant load resister value.

It is observed that at a constant output voltage V_{out} , the auxiliary voltage V_{aux} varies almost linearly with the variation of the load resistors. It also varies with the variation of the output voltage for constant load resistors. The variation of the auxiliary feedback voltage with the variation of the output voltage for different values of load resistors is shown in Figure 18.

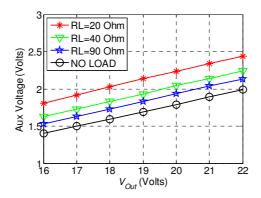


Figure 18 Variation of Vaux with Vout for different loads

At a constant output voltage the variation of V_{aux} with the variation in output load is due to a change of primary current through the power transformer. The primary winding of transformer is coupled with the auxiliary winding. Therefore any change in the load resistor will change the input current through the primary winding and hence the auxiliary voltage varies. In Figure 18 it is obvious that the auxiliary feedback voltage changes around 25% for a given output voltage at different loading conditions. With this variation, it is not possible to sense the output voltage correctly and this thus creates uncertainty in a closed loop system.

In order to correctly sense the output voltage, the input current must be measured. As shown in Figure 17 a shunt resistor R_{shunt} is used in series with the lower MOSFET to measure the input current. The variation of input current is measured under the following conditions.

- Fixed value of output voltage V_{out} and different values of load resistors.
- Variation of output voltage V_{out} and constant load resister value.

The measurement results are plotted in Figure 19. It is inferred that at constant output voltage, the input current varies almost linearly with the variation of the load resistors. For a fixed $V_{out} = 20V$, the value of the input current is different for different load resistors (20 Ω , 40 Ω and 90 Ω). For a constant value of the load resistor, the variation of the input current is linear with the variation of output voltage.

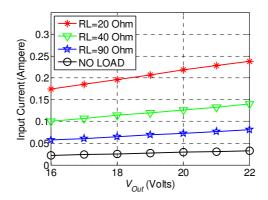


Figure 19 Variation of input current with Vout for different loads

From the measurement results of Figure 18 and Figure 19 it can be observed that in order to correctly sense the output voltage, a linear expression can be established between the input current and the auxiliary feedback voltage. The linear expression is given in Equation 3.2.

$$V_{out} = A \times V_{aux} + B \times I_{in}$$
 3.2

where A and B are constants and are selected to provide a constant value at a specified output voltage.

The output voltage V_{out} is calculated according to equation 3.2 and the results are plotted in Figure 20. The dotted line in Figure 20 shows the ideally calculated value of V_{out} as a function of the actually measured value of V_{out} . However, it can be observed that with the assistance of Equation 3.2, the calculated output voltage is nearly independent of the load resistors at a specific output voltage (20V in this case). The equation gives the worst result under no load conditions, but this is still less than a 4% error.

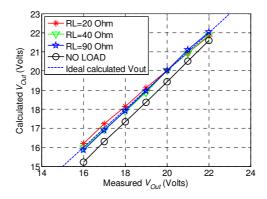


Figure 20 Measured and calculated values of V_{out}

4 FULL BRIDGE CONVERTER DESIGN

Full-bridge converters are mainly used in high-power applications such as motor drives, uninterruptible power supplies and switch mode transformer isolated power supplies. The schematic diagram of a full bridge converter is shown in Figure 21.

During the first half cycle, transistors S1 and S4 simultaneously turn on and off while in the second half cycle, transistors S2 and S3 simultaneously turn on and off. If both switches of one side (i.e S1 and S2) are simultaneously switched off then an output current will continuously flow, which will create non-linearity in the relationship between the control voltage and the average output voltage [36]. A short-through occurs when both the transistors of one leg (S1 and S2) are switched on simultaneously.

The voltage stress on the power switches is limited to the input voltage source value and the full input voltage appears across the primary winding. On the secondary side of the transformer, the voltage is stepped-up or stepped-down, rectified and filtered in order to produce a DC output voltage.

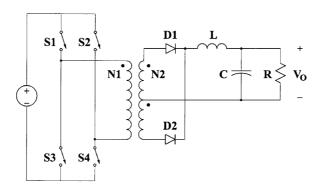


Figure 21 Full Bridge converter[5]

The operation of a full bridge is similar to that of the half bridge under steady-state conditions [5]. The output voltage V_{out} is directly related to the on state time T_{on} of the transistor. The relation is derived by integrating the inductor voltage over a time period T_s .

The average value of V_{out} is given in Equation 4.2 [5].

$$V_{out} = \frac{1}{T_s} \int_{0}^{T_s} V_{out}(t) dt = \frac{2}{T_s} \left[\int_{0}^{T_{on}} (\frac{N_s}{N_p} V_{in} - Vout) dt + \int_{T_s/2}^{T_s/2 + DT_s} - V_{out} dt \right]$$

$$4.1$$

$$V_{out} = 2\frac{N_s}{N_n} V_{in} D \tag{4.2}$$

where
$$D = \frac{T_{on}}{T_{s}}$$

Since the full bridge converter consists of four power switches, four drivers are thus required to drive the power switches. The design of a full bridge is more complex than that of a half bridge converter.

4.1 SIMULATION MODEL

The simulation design of the high frequency full bridge DC to DC converter with the high frequency circuit model of the coreless PCB step-up transformer is shown in Figure 22. The transformer primary windings are connected to the full bridge converter output, while the center tapped secondary windings of the transformer are connected to a full wave rectifier circuit. The converter circuit is simulated in the frequency range from 1MHz to 4MHz, and the energy efficiency of the open loop converter is calculated. At 2.5 MHz switching frequency, 9V input voltage 35% duty cycle and 160 Ω load resistor, the energy efficiency obtained in simulation is approximately 82%.

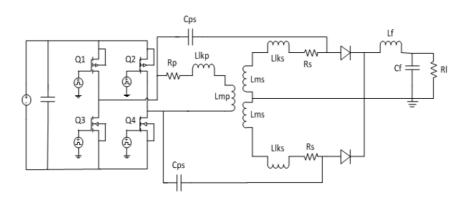


Figure 22 Schematic diagram of full bridge converter

4.2 HARDWARE IMPLEMENTATION AND MEASUREMENT RESULTS

A full bridge step-up converter circuit is implemented on a PCB. A DSPIC33fJ016GS502 microcontroller is used in the converter in order to generate PWM signals that are fed to a MOSFET driver. Since the MOSFETs are operated at low voltage, no isolation is thus used for the high side MOSFETs and the gate signals are directly fed to all MOSFETs. The FDS8958 dual N- and P-Channel enhancement mode power FETs are used in the design. They have a 30V Drain-Source Voltage and a 2Watt Power dissipation

for dual operation [37]. On the secondary side of the power transformer, a Schottky rectifier diode "20CWT10FN" is used. It has a reverse voltage blocking capability of 100V and a forward rectified current capability of 10A.

The energy efficiency of the unregulated full bridge converter circuit is computed for the input DC voltage of up-to 9 V, 35% duty cycle and switching frequency in the range of 1 to 4 MHz, with the load resistances of 160 Ω . The maximum power achieved in this design is 5.39W. The variation of energy efficiency with the variation switching frequency is shown in Figure 23. It can be observed that as the switching frequency increases beyond 2.4 MHz, the switching losses increase and the energy efficiency degrades.

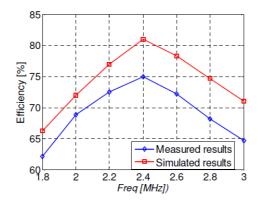


Figure 23 Variation of energy efficiency with the variation of switching frequency

4.3 PARAMETERS OF PCB TRANSFORMER USED IN FULL BRIDGE CONVERTER

A coreless PCB center-tapped step-up power transformer with a turns ratio of 1:4 designed at Mid Sweden University is used for the full bridge converter. It can be operated in the 1 to 4 MHz frequency region with energy efficiency greater than 90%. The outer diameter of the PCB power transformer is 36mm and the distance between the two consecutive layers of the PCB is 0.4mm. The transformer structure has two secondary windings in the first and the fourth layers while there are two primary windings in the second and third layers for achieving a better coupling between the primary and secondary windings. The secondary windings are connected in series and the primary windings are connected in parallel to achieve the desired inductance. The parameters of the step-up transformer used in the full bridge converter are as follows:

- The self-inductances of the primary and secondary winding are 1.275μH and 10.45μH respectively.
- The leakage inductances of the primary and secondary winding are 0.326μH and 2.86μH respectively.

- The AC resistance of primary and secondary winding of the transformer are 0.27Ω and 2.3Ω respectively.
- The inter-winding capacitance is approximately 101pF.

The energy efficiency with a sinusoidal excitation of the transformer is shown in Figure 24

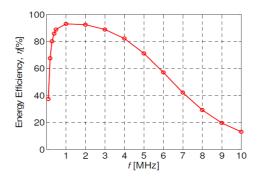


Figure 24 Energy efficiency of the coreless PCB power transformer

4.4 DESIGN LIMITATIONS

The total losses of the full bridge converter are shared by the MOSFETs, transformer and diodes. The coreless PCB transformer in the converter design has shown major contribution in attaining both a high energy efficiency and compactness. At higher switching frequencies, the switching loss in the power MOSFET becomes significant. This places a limit in attaining high power levels and a high efficiency in the converter design. The temperature profile of the power MOSFETs at a power level of 5W, recorded using an IR thermal camera, is shown in Figure 25.

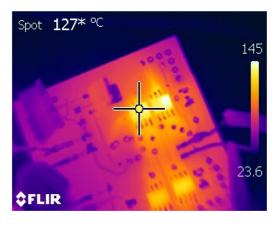


Figure 25 Thermal profile of MOSFETs

5 THESIS SUMMARY AND CONCLUSIONS

Chapter 1: The basic introduction of linear and switch mode power supplies is given. The advantages and disadvantages of both the power supplies are discussed. The motivating factors for a high frequency SMPS design, such as the high frequency power MOSFETs, PCB transformers and smaller EMI filters are discussed. It can stated that, with the improvement in power MOSFET technology and the development of high frequency multilayered PCB power transformers, it is now possible to design high frequency and power efficient isolated converters. Although the size of SMPS can be decreased by increasing the switching frequencies but there are certain challenges in the design of high frequency switching converters. These challenges are discussed in this chapter.

Chapter 2: In this chapter the design of a half bridge DC-DC converter is discussed. The theoretical background and the basic operating principle of a half bridge converter circuit and its transformer design are discussed. A simulation model and the hardware implementation of a high frequency half bridge converter are also presented. The PCB step down power transformer is used in the converter. A PCB isolation transformer is also used for providing the isolated gate signals for the high side MOSFETs. The parameters and energy efficiency of both transformers are given. The maximum energy efficiency of the PCB step down power transformer used in the design is 96% at a switching frequency of 2.6 MHz. The energy efficiency of the converter of the converter is measured up to a 40W output power. The converter is switched up to 3 MHz switching frequencies. The maximum energy efficiency is approximately 82%. This work is a preliminary step in the design of forward converters in the MHz frequency region and the losses in a converter are estimated.

Chapter 3: Two feedback techniques are implemented in the half bridge converter which was presented in chapter 2. Measurement results for both the feedback techniques are analysed. It is observed that, although the output voltage can be predicted with the use of an opto-coupler feedback, this opto-coupler feedback is temperature sensitive and is relatively expensive. The feasibility of a feedback signal, using the auxiliary winding of a coreless PCB power transformer, is discussed. It is observed that in order to accurately predict the output voltage with auxiliary feedback, the primary current must be measured in combination with the auxiliary voltage. Both the auxiliary feedback voltage and the input current vary linearly with the variation of the output voltage. Therefore, a linear mathematical expression is established between the auxiliary feedback voltage and the input current in order to calculate the output voltage based on the variation of the input current and the auxiliary voltage.

Chapter 4: In this chapter the design of a full bridge DC-DC converter is discussed. A brief theoretical background and the basic operating principle of a full bridge converter circuit and its transformer design are discussed. A simulation model and the hardware implementation of the converter are described. The measurement and simulation results of the converter are presented. The maximum energy efficiency of 82% has been achieved in

the simulation circuit while, in the actual hardware circuit a maximum energy efficiency of 72% has been achieved. A coreless PCB step up power transformer designed at Mid Sweden University is used in the implementation of the converter circuit. In switching the frequency range of 1-4 MHz, a maximum energy efficiency of 90% has been achieved for the power transformer. The limitations of the converter are discussed.

5.1 FUTURE WORK

The EMI is a very important issue for almost all electronic equipments. The increased switching frequency, in combination with sudden changes in the current (di/dt) or voltage(dv/dt) levels generates higher order harmonics, which causes EMI and affects the Electro Magnetic Compatibility (EMC) of the SMPS.

The EMC design is a very important requirement for SMPS. Therefore it is essential to limit the EMI so that the product is developed according to EMC standards. To achieve this, there are many approches such as filtering, shielding and isolation etc. Future work will be focused on the design of one or two stage EMI filters for DM and CM noise attenuation in high frequency power supplies. The filters will be characterized and their signal behaviour will be studied.

6 PAPER SUMMARY

6.1 HIGH FREQUENCY HALF-BRIDGE CONVERTER USING MULTILAYERED CORELESS PRINTED CIRCUIT BOARD STEP-DOWN POWER TRANSFORMER

A compact and high density half bridge DC-DC converter is designed and tested by the implementation of the circuit on a printed circuit board. The converter is operated in the MHz frequency region with a maximum output power of 40 W. The maximum energy of the unregulated converter was approximately 82 %. The maximum energy efficiency as a function of input voltage, duty cycle and switching frequency was computed. Multilayered coreless PCB transformers used in the converter circuit have provided a major contribution in both the energy efficiency and its compactness. It is observed that in the future, it will be possible to design very small and compact switch mode power supplies once better switching devices and techniques have been developed.

6.2 ANALYSIS OF FEEDBACK IN CONVERTER USING CORELESS PRINTED CIRCUIT BOARD TRANSFORMER

In this paper, the feasibility of a feedback signal, using the auxiliary winding of a coreless PCB power transformer, is discussed. Both opto-coupler and auxiliary feedback voltages are implemented, measured and analyzed. Although the opto-coupler feedback voltage remains constant for a given output voltage for different loads, the implementation of opto-coupler feedback remains temperature sensitive and has a relatively high cost.

To accurately sense the output voltage with auxiliary feedback, the primary current is also measured in combination with the auxiliary voltage. A mathematical expression is established to calculate the output voltage with the variation of the input current and the auxiliary voltage. This expression provides good results for different loads, while, under no load conditions, it offers an error less of than 4%, which is quite acceptable in many cases.

It is observed from the analysis that the auxiliary feed-back can be used as a feed-back control loop for a high frequency half-bridge DC-DC converter as a better alternate than the opto-coupler feedback because it is simple to implement, insensitive to temperature variations and is cost effective.

6.3 HIGH FREQUENCY FULL BRIDGE CONVERTER USING MULTILAYER CORELESS PRINTED CIRCUIT BOARD STEP UP POWER TRANSFORMER PLATFORM

In this paper the design of a full bridge DC to DC converter using a multilayer coreless PCB step-up power transformer is discussed. The design of the converter is tested up to 5 to 6Watts. The measured energy efficiency of the unregulated converter is 75% at 2.4MHz frequency. The major loss contribution in the design was due to the switches. This places a limit on attaining high power levels and high efficiency in such a converter design. The coreless PCB transformer in the converter design has provided a major contribution in attaining high energy efficiency and compactness. Better switching devices with high

power dissipation level in the required voltage/current range can improve both the power level and the efficiency of the converter.

6.4 AUTHORS' CONTRIBUTIONS

The exact contributions of the authors of the three central papers in this thesis are summarized in Table 6-1.

Table 6-1. Authors' Contributions

| Paper # | Main author | Co-authors | Contributions |
|---------|-------------|----------------------------|---|
| I | AM | HK JS RA SH KB | AM: Literature study, design, implementation and detailed analysis HK: Design of gate drive circuitry, discussion and review of paper. JS: Help in implementation, discussion and review. RA: Power and signal transformer design, secondary inductor design and parameters extraction and transformer characterisation. KB: Supervision of the implementation work and final review of paper |
| П | AM | JS HK RA SH KB | AM: Literature study, design, implementation and detailed analysis JS: Help in measurements, discussion and review. HK: Discussion and review of paper. RA: Transformer design, discussion and review of paper. SH: Help in design of auxiliary Feedback Circuit KB: Supervision of the implementation work and final review of paper |
| III | JS | AM RA HK KB | JS: Literature study, Design, implementation and detailed analysis. AM: Testing, analysis, discussion and review. RA: Power transformer design, secondary inductor design and parameters extraction. HK: Discussion and review of paper KB: Supervision of the implementation work and final review of paper |

- 1. Abdul Majid (AM)
- 2. Kent Bertilsson (KB)
- 3. Jawad Saleem (JS)
- 4. Hari Babu Kotte (HK)
- 5. Radhika Ambatipudi (RA)
- 6. Stefan Haller (SH)

REFERENCES

- [1] Abraham Pressman, Keith Billings, Taylor Morey "Switching Power Supply Design", third edition.
- [2] Marty Brown, "Power supply cookbook", second edition
- [3] Hari Babu Kotte, "High Speed (MHz) Switch Mode Power Supplies(SMPS) using Multilayered Coreless PCB Transformer technology Passive gate drive circuit using Coreless Printed Circuit Board (PCB) Signal Transformer", Licentiate Thesis 62, Mid Sweden University, ISSN: 1652-8948, ISBN: 978-91-86694-41-8
- [4] "Design of Transformers for Switched Mode Power Supplies", Version 2 EE IIT, Kharagpur Module 3 lesson 25
- [5] Muhammad H. Rashid book "Power Electronics Handbook", Academic Press
- [6] Eberle, W.; Zhiliang Zhang; Yan-Fei Liu; Sen, P.C.; , "A Current Source Gate Driver Achieving Switching Loss Savings and Gate Energy Recovery at 1-MHz," *Power Electronics, IEEE Transactions on*, vol.23, no.2, pp.678-691, March 2008
- [7] L. Lorenz, G. Deboy, A. Knapp and M. März, "COOLMOSTM "A new milestone in high voltage Power MOS", Siemens AG, Semiconductor Division, Balanstr. 73, 81541 Munich, Germany
- [8] Ashot Melkonyan, "High Efficiency Power Supply using new SiC devices" PhD thesis published by University of Kassel February 09, 2007.
- [9] Khan, M.A.; Simin, G.; Pytel, S.G.; Monti, A.; Santi, E.; Hudgins, J.L.; , "New Developments in Gallium Nitride and the Impact on Power Electronics," *Power Electronics Specialists Conference*, 2005. PESC '05. IEEE 36th , vol., no., pp.15-26, 16-16 June 2005
- [10] Radhika Ambatipudi, Hari Babu Kotte and Kent Bertilsson, "Coreless Printed Circuit Board (PCB) Step-down Transformers for DC-DC Converter Applications," *Proceedings of World Academy of Science, Engineering and Technology*, Vol.70, pp 380-389, ISSN: 1307-6892, October 2010, Paris
- [11] Bob Stove, "A tutorial on Power Semiconductor Switches", http://www.truepowerresearch.com/2011/03/tutorial-power-semiconductor-switchespower-mosfets-and-schottky-diodes/ (last accessed January 10, 2012)
- [12] Maurizio Granato and Roberto Massolini "The GaN Opportunity-Higher Performances and New Challenges" www.power-mag.com Issue 6, 2011
- [13] Radhika Ambatipudi, Hari Babu Kotte and Kent Bertilsson,"Comparison of Two Layered and Three Layered Coreless Printed Circuit Board (PCB) Step-Down Transformers", Proceedings of *The 3rd International Conference on Power Electronics and Intelligent Transportation System* (PEITS 2010), November 20-21, Shenzhen, China
- [14] N. Z. Yahaya, IAENG, K. M. Begam, and M. Awan "A Review on VHF Power Electronics Converter and Design Issues" Engineering Letters, 16:3, EL_16_3_03
- [15] Bob Bell, "Half-bridge topology finds high density power converter apps", http://www.powerdesignindia.co.in/STATIC/PDF/200810/PDIOL_2008OCT24_PMNG_TA_03.pdf? (last accessed December 22, 2010)
- [16] Colonel Wm. T. McLyman, "Designing Magnetic components for high frequency DC-DC converters"
- [17] Fu Keung Wong, "High Frequency Transformers for Switch Mode Power Supplies", PhD thesis March 2004
- [18] Tang, S.C.; Hui, S.Y.; Henry Shu-Hung Chung; , "Coreless planar printed-circuit-board (PCB) transformers-a fundamental concept for signal and energy transfer," *Power Electronics, IEEE Transactions on* , vol.15, no.5, pp.931-941, Sep 2000
- [19] Tang, S.C.; Hui, S.Y.R.; Chung, H.S.-H.; , "A low-profile power converter using printed-circuit board (PCB) power transformer with ferrite polymer composite," *Power Electronics, IEEE Transactions on* , vol.16, no.4, pp.493-498, Jul 2001

- [20] Radhika Ambatipudi, "Multilayered Coreless Printed Circuit Board (PCB) Step-down Transformers for High Frequency Switch Mode Power Supplies (SMPS)", Licentiate Thesis 61, Mid Sweden University, ISSN: 1652-8948, ISBN: 978-91-86694-40-1
- [21] Hari Babu Kotte, radhika Ambatipudi and kent Bertilsson, "High Speed Series Resonant Converter(SRC) Using Multilayered Printed Circuit Board Step-Down Power Transformer", Proceedings of 33rd International Telecommunications Energy Conference (INTELEC 2011).
- [22] Datasheet of "dsPIC33Fj16GS502" from Microchip, http://www.microchip.com/wwwproducts/Devices.aspx?dDocName=en537164(Last accessed January 22, 2012)
- [23] Data sheet of SPU02N60S5 Cool MOS Power Transistor Infineon Technologies AG, "http://www.alldatasheet.com/datasheet-pdf/pdf/419235/INFINEON/SPU02N60S5.html"
- [24] Data sheet of Schottky barrier rectifier diode SR-1660, http://www.datasheetcatalog.com/datasheets_pdf/S/R/1/6/SR1660.shtml(Last accessed January 22, 2012)
- [25] Majid, A.; Kotte, H.B.; Saleem, J.; Ambatipudi, R.; Haller, S.; Bertilsson, K.; , "High frequency half-bridge converter using multilayered coreless Printed Circuit Board step-down power transformer," *Power Electronics and ECCE Asia (ICPE & ECCE)*, 2011 IEEE 8th International Conference on , vol., no., pp.1177-1181, May 30 2011-June 3 2011
- [26] Dr. Dušan Graovac, MarcoPürschel, Andreas Kiep MOSFET Power Losses Calculation Using the Data-Sheet Parameters", Application Note, V 1.1, July 2006
- [27] John Shen, Z.; Yali Xiong; Xu Cheng; Yue Fu; Kumar, P.; , "Power MOSFET Switching Loss Analysis: A New Insight," *Industry Applications Conference*, 2006. 41st IAS Annual Meeting. Conference Record of the 2006 IEEE , vol.3, no., pp.1438-1442, 8-12 Oct. 2006
- [28] Ron Lenk, "Practical design of power supplies", JOHN WILEY & SONS, INC., PUBLICATION pp 169-170.
- [29] Carl Keith Sawtell, Paolo Menegoli, "Power Supply Control Circuit with optical feedback", US Patent No. 7800037B2, September 21, 2010.
- [30] George Barbehahenn; Hustan W Rice, "Simplified AC-DC Switching converters with output isolation." US Patent No. 5914865 June 22, 1999.
- [31] Irving, B.T.; Jovanovic, M.M.; , "Analysis and Design Optimization of Magnetic-Feedback Control Using Amplitude Modulation," Power Electronics, IEEE Transactions on , vol.24, no.2, pp.426-433, Feb. 2009
- [32] Che-Wei Chang, Yu-Tzung Lin, and Ying-Yu Tzou, "Digital Primary-Side Sensing Control for Flyback Converters", *The eighth International Conference on Power Electronics and Drive Systems (PEDS 2009)*
- [33] "Optoelectronic Feedback Control Techniques for Linear and Switch Mode Power Supplies", Application Note 55, Vishay Semiconductors
- [34] Data sheet of "IL205A" Phototransistor opto-coupler, http://www.datasheetarchive.com/IL205A-datasheet.html (Last accessed January 22, 2012)
- [35] Ta-yung Yang, Chern-Lin Chen, Jenn-yu G.Lin, Yi-Hsin Leu, "PWM Controller Regulating Output Current in Primary Side" US 6721192B1 April 13, 2004
- [36] N. Mohan, T. Undeland, and W. P. Robbins, Power Electronics. New York: Wiley, 1995
- [37] FDS8958A Datasheet www.fairchildsemi.com/ds/FD/FDS8958A.pdf (Last accessed November 25, 2011
- [38] Hari Babu Kotte, Radhika Ambatipudi and Kent Bertilsson, "A ZVS Flyback DC-DC Converter Using Multilayered Coreless Printed-Circuit Board (PCB) Step-down Power Transformer," Proceedings of World Academy of Science, Engineering and Technology, Vol.70, pp 148-155, ISSN: 1307-6892, October 2010, Paris.
- [39] Dongbing Zhang, Dan Y. Chen, Senior Member, IEEE, Mark J. Nave, and Dan Sable "Measurement of Noise Source Impedance of Off-Line Converters"